

 Open access • Journal Article • DOI:10.1063/1.448381

Quantum Monte Carlo calculation of the singlet–triplet splitting in methylene

— [Source link](#) 

Peter Reynolds, Michel Dupuis, William A. Lester, William A. Lester

Institutions: Lawrence Berkeley National Laboratory, Pacific Northwest National Laboratory, University of California, Berkeley

Published on: 15 Feb 1985 - Journal of Chemical Physics (American Institute of Physics)

Topics: Quantum Monte Carlo

Related papers:

- [Fixed-node quantum Monte Carlo for molecules](#)
- [Quantum Monte Carlo for molecules: Green's function and nodal release](#)
- [H + H₂ reaction barrier: A fixed-node quantum Monte Carlo study](#)
- [Quantum Monte Carlo calculations on Be and LiH](#)
- [A random-walk simulation of the Schrödinger equation: H+3](#)

Share this paper:    

View more about this paper here: <https://typeset.io/papers/quantum-monte-carlo-calculation-of-the-singlet-triplet-ou9eyx8oi8>

Lawrence Berkeley National Laboratory

Recent Work

Title

QUANTUM MONTE CARLO CALCULATION OF THE SINGLET-TRIPLET SPLITTING IN METHYLENE

Permalink

<https://escholarship.org/uc/item/2cn8j2hp>

Author

Lester, W.A.

Publication Date

1984-08-01



Lawrence Berkeley Laboratory

UNIVERSITY OF CALIFORNIA RECEIVED

Materials & Molecular Research Division

LAWRENCE
BERKELEY LABORATORY

DEC 19 1984

LIBRARY AND
DOCUMENTS SECTION

Submitted to the Journal of Chemical Physics

QUANTUM MONTE CARLO CALCULATION OF THE
SINGLET-TRIPLET SPLITTING IN METHYLENE

P.J. Reynolds, M. Dupuis, and W.A. Lester, Jr.

August 1984

TWO-WEEK LOAN COPY
*This is a Library Circulating Copy
which may be borrowed for two weeks.*



LBL-17823
e.2

DISCLAIMER

This document was prepared as an account of work sponsored by the United States Government. While this document is believed to contain correct information, neither the United States Government nor any agency thereof, nor the Regents of the University of California, nor any of their employees, makes any warranty, express or implied, or assumes any legal responsibility for the accuracy, completeness, or usefulness of any information, apparatus, product, or process disclosed, or represents that its use would not infringe privately owned rights. Reference herein to any specific commercial product, process, or service by its trade name, trademark, manufacturer, or otherwise, does not necessarily constitute or imply its endorsement, recommendation, or favoring by the United States Government or any agency thereof, or the Regents of the University of California. The views and opinions of authors expressed herein do not necessarily state or reflect those of the United States Government or any agency thereof or the Regents of the University of California.

QUANTUM MONTE CARLO CALCULATION OF THE SINGLET-TRIPLET SPLITTING IN METHYLENE *

Peter J. Reynolds, Michel Dupuis, [†] and William A. Lester, Jr. [‡]Materials and Molecular Research Division
Lawrence Berkeley Laboratory
University of California
Berkeley, California 94720**Abstract**

The fixed-node quantum Monte Carlo (QMC) method is used to calculate the total energy of CH₂ in the ³B₁ and ¹A₁ states. For both states, the best QMC variationally bounded energies lie more than 15 kcal/mole (0.024 h) below the best previous variational calculations. Subtracting these energies to obtain the singlet-triplet splitting yields $T_e = 9.4 \pm 2.2$ kcal/mole. Adjusting for zero-point energies and relativistic effects, we obtain $T_0 = 8.9 \pm 2.2$ kcal/mole. This result is in excellent agreement with the recent direct measurements of McKellar *et al.* of $T_0 = 9.05 \pm 0.06$ kcal/mole, and of Leopold *et al.* of ~ 9 kcal/mole, as well as with recent theoretical investigations which indicate an energy gap of 9-11 kcal/mole. We summarize the QMC method, discuss a possible scheme for iteratively correcting the procedure, and note that the present results were obtained using only single determinant functions for *both* states, in contrast to conventional *ab initio* approaches which must use at least two configurations to properly describe the singlet state.

* A preliminary account of this work was presented at the 17th Annual Sanibel Symposium, March 1983. This work was supported in part by the Office of Naval Research, by the Director, Office of Energy Research, Office of Basic Energy Sciences, Chemical Sciences Division of the U. S. Department of Energy under Contract No. DE-AC03-76SF00098, and by the Control Data Corporation under Grant No. 82-CSU-12.

[†] Present address: IBM Research Laboratory, Kingston, N. Y. 12401.

[‡] Also, Department of Chemistry, University of California, Berkeley, CA 94720.

I. Introduction

The methylene molecule has been studied extensively over the past two decades, both experimentally and theoretically. It is a highly reactive radical, whose chemistry depends significantly on which of two closely spaced, low-lying states it is found in. Photochemical reactions, frequently used to produce CH_2 , create it in both states. Methylene was first observed by Herzberg¹. He detected both the $^1\text{A}_1$ and $^3\text{B}_1$ states in absorption spectra, and he concluded that the triplet is the ground state. Thus it has been of long-standing experimental interest to determine T_0 , the energy difference between these two lowest levels. On the other hand, the small size of CH_2 makes it amenable to thorough investigation by theoretical methods. Hence a calculation of the singlet-triplet splitting can serve as an excellent test of the reliability of various calculational procedures.

Early calculations, however, disagreed strongly with early experiments. Theory² predicted a splitting of 30 kcal/mole, while experiment³ indicated only 1-2 kcal/mole. Over the last decade, refinements of theoretical techniques have led to a value which has steadily fallen, with numerous *ab initio* results converging to about 10-11 kcal/mole⁴. Experiments of improved sophistication⁵, on the other hand, gradually obtained increasing values, reaching 8-10 kcal/mole by around 1976. Agreement appeared forthcoming. In 1976, however, the first direct measurement of the singlet-triplet splitting (one which made no recourse to thermodynamic assumptions) obtained 19.5 kcal/mole using photoelectron spectroscopy⁶. This new disagreement spurred more experiments and more theory. On the experimental side, careful re-examination⁷ of the earlier direct measurement⁶ reaffirmed the value of 19.5 kcal/mole. However, laser-induced fluorescence experiments⁸ and measurements of fragment velocities in ketene photodissociation in a molecular beam⁹ gave 8.1 and 8.5 ± 0.8 kcal/mole respectively. Furthermore, very recent direct laser-magnetic resonance spectroscopy

experiments¹⁰ have yielded $T_0 = 9.05 \pm 0.06$ kcal/mole. Finally, a new experimental reinvestigation of this problem by Lineberger and coworkers appeared³⁴ after the present paper was substantially completed. That work identifies their previous results as due to vibrational hot bands in the photoelectron spectrum, and indicates an energy gap of ~ 9 kcal/mole. On the theoretical side, workers were unable to find any indication of a splitting as large as 19.5 kcal/mole. Theory ultimately has come to favor values in the range of 9-11 kcal/mole¹¹, with *ab initio* values in the 10-11 kcal/mole range⁴. Semi-empirical corrections to the latter are required to achieve 9 kcal/mole¹¹. Thus now it again appears that theory and experiment are in good accord, though a possible discrepancy of 1-3 kcal/mole remains with *ab initio* calculations.

Since all the above-mentioned theoretical calculations have in common the familiar *ab initio* approaches (e.g. SCF, MCSCF, CI), it is of interest to compute the level splitting by a totally independent method. To this end we have employed the quantum Monte Carlo (QMC) approach¹²⁻²⁴, which has demonstrated high accuracy in trial calculations to date. The essence of the method is summarized in Sec. II. Further, in Sec. III we describe an iterative scheme that may have potential for improving the method. We present and discuss our results on CH₂ in Sec. IV, and relate our findings to experiment in Sec. V. Our best determination for the singlet-triplet splitting, corrected for zero-point and relativistic effects is $T_0 = 8.9 \pm 2.2$ kcal/mole. The error bars are statistical (due to the Monte Carlo approach) and indicate one standard deviation in a normal distribution. This result disagrees strongly with the direct measurements of Refs. 6,7; however, QMC is in good agreement with the recent experiments^{9,10,34} discussed above.

II. Quantum Monte Carlo Approach

In the past few years, Monte Carlo approaches have seen increased application in a number of diverse fields. Recently, quantum mechanical Monte Carlo (QMC) methods¹²⁻²⁴ have been successfully used for the treatment of molecular problems^{14,16,19-23}. What we mean here by QMC is a Monte Carlo procedure which "solves" the Schrödinger equation. (This is to be distinguished from so-called variational Monte Carlo, in which one obtains expectation values for a *given* trial wave function.)

Briefly, the procedure is to simulate the quantum system by allowing it to evolve under the time-dependent Schrödinger equation in imaginary time. It is easy to show¹⁹ that the use of imaginary time causes the system to approach a stationary state which is the lowest state of a given symmetry. Properties may then be "measured" as averages over the resulting equilibrium distribution. Until now only ground-state properties have been so obtained.

The various QMC approaches differ somewhat in their details²⁴. The method we use here is the fixed-node, diffusion QMC. For a full discussion see Refs. 18 and 19. The following overview, however, presents the essence of the method.

By writing the imaginary-time Schrödinger equation with a shift in the zero of energy as

$$\frac{\partial \Psi(\underline{R}, t)}{\partial t} = D \nabla^2 \Psi(\underline{R}, t) + [E_T - V(\underline{R})] \Psi(\underline{R}, t) , \quad (1)$$

we immediately see that it may be interpreted as a generalized diffusion equation. The first term on the right-hand-side is the ordinary diffusion term, while the second term is a position-dependent rate (or branching) term. For an electronic system, $D = \hbar^2 / 2m_e$, \underline{R} is the three-N dimensional coordinate vector of the N electrons, and $V(\underline{R})$ is the Coulomb potential. Since diffusion is the continuum limit of a random walk, one may simulate Eq. (1) with the function Ψ (note, *not* Ψ^2) as the density of "walks". The walks undergo an exponential birth and

death as given by the rate term. This connection between a quantum system and a random walk was first noted by Metropolis, who attributes it to Fermi²⁵.

The steady-state solution to Eq. (1) is the time-independent Schrödinger equation. Thus we have $\Psi(\underline{R}, t) \rightarrow \varphi(\underline{R})$, where φ is an energy eigenstate. The value of E_T at which the population of walkers is asymptotically constant gives the energy eigenvalue. Calculations employing Eq. (1) in this way were done by Anderson on a number of one to four electron systems¹⁴.

Unfortunately, in order to treat systems larger than two electrons, the Fermi nature of the electrons must be taken into account. The antisymmetry of the eigenfunction implies that Ψ must change sign; however, a density (e.g. of walkers) cannot be negative. To handle this, Anderson¹⁴ made simplifying assumptions about the positions of the nodes. This method is *ad hoc*, and not readily generalizable. Another method which imposes the antisymmetry, and at the same time provides more efficient sampling (thereby reducing the statistical "noise"), is importance sampling^{19,18,19} with an antisymmetric trial function Ψ_T . The zeroes (nodes) of Ψ_T become absorbing boundaries for the diffusion process, which maintains the antisymmetry. The additional boundary condition that Ψ vanish at the nodes of Ψ_T is the fixed-node approximation¹⁷. The magnitude of the error thus introduced depends on the quality of the *nodes* of $\Psi_T(\underline{R})$, and vanishes as Ψ_T approaches the true eigenfunction. To the extent that Ψ_T is a good approximation of the wave function, the true eigenfunction is almost certainly quite small near the nodes of Ψ_T . Thus one expects the fixed-node error to be small for reasonable choices of Ψ_T . Previous work on a number of systems has borne this out^{19,20,22}. In addition, this error is variationally bounded^{18,19}. Algorithmic approaches also exist which "release" the nodal constraint, though at the cost of an unbounded increase in the variance.^{17,23,24} Since the fixed-node approximation has been found to be adequate in most situations^{19,20,22} (see also Sec. V), we use it here.

To implement importance sampling and the fixed-node approximation, Eq. (1) is multiplied on both sides by Ψ_T , and rewritten in terms of the new probability density $f(\underline{R},t) = \Psi_T(\underline{R})\Psi(\underline{R},t)$. The resultant equation for $f(\underline{R},t)$ may be written

$$\frac{\partial f}{\partial t} = D\nabla^2 f + [E_T - E_L(\underline{R})]f - D\nabla \cdot [f F_Q(\underline{R})] . \quad (2)$$

The local energy $E_L(\underline{R})$, and the "quantum force" $F_Q(\underline{R})$ are simple functions of Ψ_T given by

$$E_L(\underline{R}) \equiv H\Psi_T(\underline{R}) / \Psi_T(\underline{R}) , \quad (3a)$$

and

$$F_Q(\underline{R}) \equiv 2\nabla\Psi_T(\underline{R}) / \Psi_T(\underline{R}) . \quad (3b)$$

Equation (2), like Eq. (1) is a generalized diffusion equation, though now with the addition of a drift term due to the presence of F_Q .

In order to perform the random walk implied by Eq. (2) we use a short-time approximation to the Green's function which is used to evolve $f(\underline{R},t) \rightarrow f(\underline{R}',t+\tau)$. This process is iterated¹⁹ to large t . Such an approach becomes exact in the limit of vanishing time-step size, τ . We discuss the time-steps used and the error so introduced in Sec. V. There is also an exact Green's function approach^{21,23,24}.

In earlier QMC work^{19,20} it was demonstrated for a number of 2-10 electron molecules that one could obtain exceptionally accurate ground-state total energies. These energies were more accurate than the best values obtained from *ab initio* CI procedures in every case. However, one also needs to be able to calculate accurate energy *differences*, such as binding energies, barriers to chemical reaction, and level splittings. This is a far more difficult task for Monte Carlo, since a statistical uncertainty of as little as 0.1% in the total energy can mask the sought-after energy difference. To reduce the statistical error to the level needed by "brute force" is costly in computer time, as the standard deviation

decreases only as $(CPU\ time)^{-1/2}$. Algorithmic developments, such as the differential QMC²⁶, hold promise for reductions in variance through correlated sampling techniques. Another approach is based on noting that the variance decreases as Ψ_T better approximates the true eigenfunction. Thus an iterative procedure for improving Ψ_T could be helpful. If this also resulted in an improvement in the nodal positions, one would minimize the fixed-node error as well. We describe an approach along this direction in the next section.

III. Iterating Ψ_T Through Wave Function Scaling

What is a "good" choice of Ψ_T ? In practice one wants a trial function which is as simple as possible, since it will require repeated evaluation at each step of the random walk. Yet one wants a function which provides accurate results. Anderson's early work¹⁴ had no importance sampling. This corresponds to choosing $\Psi_T = 1$! Accurate results were nevertheless forthcoming, since QMC solves the Schrödinger equation *regardless* of the choice of Ψ_T . However as we noted in Sec. II, for Fermi systems inaccurate nodes in Ψ_T will lead to a small error when the fixed-node approximation is used. Furthermore, the statistical "noise" will be large for a poor choice of Ψ_T .

We have found in previous work^{19,22} that a *single determinant* Ψ_T with only a double-zeta basis set places the nodes extremely well as determined by the quality of the computed total energies. Increasing the basis set beyond double zeta appears to offer insignificant gain in either accuracy (i.e. the fixed-node error does not noticeably decrease) or precision (the statistical uncertainty, for equal computing time, remains essentially unchanged)²². In practice we have included an electron-electron Jastrow factor²⁷ in our functions Ψ_T in order to reduce statistical fluctuations¹⁹. In some cases^{19,22} we have also included an electron-nuclear factor (cf. Sec IV). Neither factor affects the positioning of the nodes, and hence the fixed-node energies.

Since the fixed-node QMC approach involves an approximation in the placement of the nodes, and, in addition, in many applications the statistical uncertainty needs to be further reduced, it is of interest to seek a procedure for correcting Ψ_T . We present here an iterative approach for globally (rather than locally) performing this correction.

Note first that the additional boundary condition that the eigenfunction vanish at the nodes of Ψ_T will generally give a solution which fails to satisfy the virial theorem. Thus the fixed-node expectation value of V is not exactly $-2T$. (Here we assume an equilibrium geometry.) We may therefore consider the fixed-node eigenfunction, which we shall denote $\hat{\varphi}(\{\mathbf{r}_i\})$, as a variational function which may be further optimized by scaling²⁸. In our notation, the caret indicates that $\hat{\varphi}$ carries the fixed-node constraint, and $\{\mathbf{r}_i\}$ indicates the set of *all* coordinates.

Let us define

$$V(1) \equiv \langle \hat{\varphi}(\{\mathbf{r}_i\}) | V | \hat{\varphi}(\{\mathbf{r}_i\}) \rangle, \quad (4a)$$

$$T(1) \equiv \langle \hat{\varphi}(\{\mathbf{r}_i\}) | T | \hat{\varphi}(\{\mathbf{r}_i\}) \rangle, \quad (4b)$$

and the scaled quantities $V(\eta)$ and $T(\eta)$ analogously in terms of the scaled function $\hat{\varphi}(\eta\{\mathbf{r}_i\})$. The expressions in Eq. (4) must of course be divided by $\langle \hat{\varphi}(\{\mathbf{r}_i\}) | \hat{\varphi}(\{\mathbf{r}_i\}) \rangle$ if $\hat{\varphi}$ is not normalized. It is readily established²⁸ that $V(\eta) = \eta V(1)$ since the Coulomb potential scales as $1/r$. Similarly, $T(\eta) = \eta^2 T(1)$ since ∇^2 scales as $1/r^2$. Combining these expressions one obtains

$$E(\eta) = \eta V(1) + \eta^2 T(1) \quad (5)$$

Varying Eq. (5) with respect to η minimizes $E(\eta)$ at

$$\eta = -V(1)/2T(1) \quad (6a)$$

and

$$E(\eta) = -V(1)^2/4T(1) \quad (6b)$$

Thus the function $\hat{\varphi}(\eta\{\tau_i\})$ has a lower variational energy than $\hat{\varphi}(\{\tau_i\})$, and in addition satisfies the virial theorem since $-V(\eta)/2T(\eta) = -\eta^{-1}V(1)/2T(1) = 1$. Note that the global scaling has uniformly expanded or contracted the nodal surfaces originally present in Ψ_T . As we demonstrate below, these new nodes are better than the original nodes of Ψ_T . However, $\hat{\varphi}(\eta\{\tau_i\})$ is no longer an eigenfunction of the Schrödinger equation (see Appendix). Thus we may iterate the above procedure starting with the new nodes--i.e. using²⁹ a Ψ_T whose nodes are those of $\hat{\varphi}(\eta\{\tau_i\})$ (see Fig. 1.). Such a function, $\Psi_T^{(1)}$, may be obtained by replacing all coordinates $\{\tau_i\}$ in Ψ_T by $\eta\{\tau_i\}$. (Essentially this involves scaling all the orbital exponents and the inter-atomic separations.) Now starting with $\Psi_T^{(1)}$ the QMC method converges to an eigenstate $\hat{\varphi}^{(1)}(\eta\{\tau_i\})$. Because $\hat{\varphi}^{(1)}(\eta\{\tau_i\})$ has the same nodes as $\hat{\varphi}(\eta\{\tau_i\})$, $\hat{\varphi}^{(1)}$ must have the lower energy since it is the exact solution for these nodes. Again, due to the fixed-node boundary condition with the new nodes, the virial theorem may not be satisfied, resulting in $\eta' = -V/2T \neq 1$ (for $\hat{\varphi}^{(1)}$). Thus we rescale by η' to obtain $\hat{\varphi}^{(1)}(\eta'\eta\{\tau_i\})$, which has a lower variational energy and again satisfies the virial theorem. The expanded or contracted nodes may then be fed back into a $\Psi_T^{(2)}$ and the process repeated. It is expected that the sequence $\eta, \eta', \eta'', \dots$ rapidly converges to unity, so that no appreciable gains will be obtained beyond the first few iterations. Figure 1 gives a schematic illustration of this iterative procedure. Since the fixed-node energies for the sequence of functions $\hat{\varphi}(\{\tau_i\}), \hat{\varphi}^{(1)}(\eta\{\tau_i\}), \hat{\varphi}^{(2)}(\eta'\eta\{\tau_i\})\dots$ is of decreasing energy, the nodes improve upon scaling.

In order to carry out the steps described above, we need to evaluate $V(1)$ and $T(1)$ as given by Eq. (4), rather than the usual QMC "mixed averages" such as $\langle \Psi_T | H | \hat{\varphi} \rangle / \langle \Psi_T | \hat{\varphi} \rangle$. For $V(1)$, a simple weighting procedure³⁰ enables one to compute the necessary average from the distribution $|\hat{\varphi}|^2$. The mixed average, on the other hand, suffices for calculating $E(1)$ since $\hat{\varphi}$ is an eigenfunction of H . From $E(1)$ and $V(1)$ one readily obtains $T(1)$.

IV. Results and Discussion

We have performed Monte Carlo calculations for both the 3B_1 and 1A_1 states of methylene using a number of different functions for Ψ_T . The geometries have been taken from *ab initio* calculations.^{4e} In particular, for the 3B_1 state we take the C-H bond length to be 2.045 bohr and the H-C-H angle to be 132.4°. For the 1A_1 state the values are 2.110 bohr and 102.4° respectively. Our Monte Carlo results obtained at these geometries are summarized in Table I, and compared with other work in Table II. All choices of Ψ_T have in common a single determinant form multiplied by a Jastrow factor. The Ψ_T 's differ only in the basis sets used and in the explicit form of the Jastrow function. The reader is reminded that the role of Ψ_T is as an importance function for variance reduction and as a trial function for placing the nodes. This function is but a starting point from which one converges to the fixed-node solution to the Schrödinger equation $\hat{\varphi}(\{r_i\})$. Thus the form of Ψ_T is far less crucial here than, e.g. in a variational calculation.

With a single-zeta quality basis set we find that the statistical error is about a factor of two larger than that obtained with a double-zeta quality basis set, for equal computing time. In addition the calculated energy is higher by about $0.02h$, although this difference is only at the borderline of statistical significance. For these reasons we did not put very much effort into the single-zeta Ψ_T . In other QMC work²² we have also found that a single-zeta basis is inadequate; however, as discussed in Sec. III, a double-zeta basis has generally proven quite good. In fact, further improvement in basis set has led to no visible improvement in the fixed-node energy—even at the kcal/mole level!²² In the present study we have augmented the double-zeta basis by including an optimized $1s$ function placed along each of the C-H bonds. Although this lowered the SCF energy by $0.016h$ for the triplet state and $0.022h$ for the singlet, no statistically significant lowering was achieved in the QMC energy of either state (see

Table I). This confirms our earlier experience with basis sets. Since no improvement was achieved with the bond functions, we used the simpler and less expensive atom-centered double-zeta basis for most of the calculations. The large error bars in Table I for the DZ + B function (especially noticeable in the energy difference) are just the result of the significantly smaller amount of computing done with this function.

Since basis set enhancement appears of little help, and since we still seek an improved Ψ_T , we next investigate the iterative scaling procedure described in Sec. III and depicted in Fig. 1. As an approximation, we have computed $V(1)$ and $T(1)$ as "mixed" averages. Thus, Eqs (4) become

$$V(1) \approx \langle \Psi_T(\{r_i\}) | V | \hat{\varphi}(\{r_i\}) \rangle / \langle \Psi_T(\{r_i\}) | \hat{\varphi}(\{r_i\}) \rangle \quad (7a)$$

and

$$T(1) \approx \langle \Psi_T(\{r_i\}) | T | \hat{\varphi}(\{r_i\}) \rangle / \langle \Psi_T(\{r_i\}) | \hat{\varphi}(\{r_i\}) \rangle \quad (7b)$$

The derivation leading to Eq. (6) still follows as before, however now $E(\eta)$, though still a minimum, need no longer be variationally bounded. This is because in the mixed average approximation

$$E(\eta) = \langle \Psi_T(\eta\{r_i\}) | H | \hat{\varphi}(\eta\{r_i\}) \rangle / \langle \Psi_T(\eta\{r_i\}) | \hat{\varphi}(\eta\{r_i\}) \rangle \quad (8)$$

and neither the scaled Ψ_T nor the scaled $\hat{\varphi}$ is an eigenfunction of H . Thus one is not assured of finding a function φ such that $E(\eta) = \langle \varphi | H | \varphi \rangle$. In Fig. 1, as we read across any line the energy still decreases from left to right. Following the downward arrow, however, no longer must give a decrease in energy, since the mixed average $E(\eta)$, obtained from the functions in the first and third columns, need not be greater than the true energy. The results presented in Table III show that this is indeed the case. In fact, the energy gets progressively worse as we iterate the scaling with the approximate η 's. Clearly the mixed average estimate for η must be poor, and the nodes are being scaled incorrectly. As we will argue later, the true η (Eq. 6a) is probably very close to unity for our starting nodes.

Use of the mixed average to minimize $E(\eta)$, with an electron-electron Jastrow factor in Ψ_T , results in an over-contraction of the nodes. This can be understood as follows. The Jastrow factor causes the electron density to spread out in space as the electrons seek to avoid each other. Scaling Ψ_T , as one does in the mixed average, thus leads to an η which attempts to pull the overall electronic distribution back in. This is clearly useful in lowering the *variational* energy. However, this same scaling also pulls the nodal surfaces in by the same factor. The correct η , on the other hand (cf. Eqs. 4,6), is independent of the Jastrow factor, and depends only on the original nodes of Ψ_T (since $\hat{\varphi}(\{\tau_i\})$ depends only on the nodes of Ψ_T). Thus it is clearly incorrect that the presence of a Jastrow factor, which has no effect on the original nodes, should result in the nodes being pulled in on scaling. In fact, the original nodes are entirely those of the determinant obtained by the self-consistent-field approximation. Though these nodes are not exact, they are correct in an average way. Thus the actual nodal adjustment should be more subtle.

These considerations lead one to be suspicious of scaling based on the mixed averages. The correct averages of Eq. (4) appear to lead to an η very close to unity when the nodes are as good as those obtained here by SCF. Thus only a minor improvement in energy and/or variance is expected. Nevertheless, Ψ_T may be greatly improved by pulling the electron distribution back in somewhat, without moving the nodes. A simple way to accomplish this is through the use of an electron-*nuclear* Jastrow factor. Although this function leaves the nodes unchanged, the improved quality of Ψ_T results in a smoother $E_L(\underline{R})$ and thus reduces the variance in a QMC calculation.

Inclusion of the electron-nuclear Jastrow factor reduces the mixed average value of η from about 1.014 to 0.998 for the triplet state, and from 1.014 to 0.991 for the singlet state. Because the triplet Ψ_T including the electron-nuclear Jastrow factor is a very good approximation to the true wave function (which can be

well described by a single determinant), the mixed η now provides a far better estimate of the true η than above. Thus we estimate that the true η differs from unity by less than 0.2%. For the singlet state, however, the electron-nuclear Jastrow appears to overcompensate for the electron-electron term. Also, since the singlet, which has two important configurations, can not be described properly by a single determinant, the mixed average η in this case is still not a good estimate of the true η . The best procedure to follow in evaluating η would be to compute $\langle V \rangle$ from Eq. (4a) by properly reweighting the local energies³⁰. However, unless the nodes of the singlet are considerably worse than the nodes of the triplet (contrary to the numerical evidence of Table I), the true η for the singlet should also be close to unity.

To conclude this section, we address the issue of computing. Our computations were performed in part on a Digital VAX 11/780, and in part on a CDC Cyber 205. The total computation time, for all our trial functions at all the time steps used, came to the equivalent of 4 hours of Cyber 205 time per state, running our final, fully vectorized code. Actual runs, however, were performed with a continually evolving vector code on the Cyber, and a scalar code on the VAX, and thus took considerably longer. No appreciable amount of memory was required for these runs.

V. Comparison with Experiment

As shown in Table II, the QMC total energies for both the singlet and the triplet states of methylene compare favorably with CI calculations. For the best trial function, the *total energy* is correct to better than 0.008 h (5 kcal/mole) of experiment, or to 1 part in 5000. The statistical uncertainty is roughly half this value (2-2.5 kcal/mole). The remaining error may be attributed to the fixed-node and the short-time approximations.

We have examined our data closely for a systematic time-step-size effect. One can in principle obtain an unbiased estimate for the fixed-node energy by extrapolation to $\tau \rightarrow 0$. However, for the work reported here the time-step error is smaller than the statistical noise, and is thus masked by it. For this reason we do not attempt to extrapolate, and instead the results we quote are averages over the four time-step sizes used, ranging from $\tau=0.01$ down to $\tau=0.00125h^{-1}$. Thus our energy has a small time-step bias. On the other hand, an extrapolation based on four points would have a considerably larger statistical uncertainty.

Comparing our results with the line marked "expt" in Table II, we conclude that the combined fixed-node and time-step error is roughly 5 kcal/mole for both the singlet and the triplet states. This translates to a Monte Carlo accuracy of 99.98% of the total energy and 96-98% of the correlation energy. Therefore in the present application, where the time-step error is negligible, the fixed-node error is seen to be manageably small. Furthermore, this error is roughly the same--to the order of 1 kcal/mole--for the two states. This means not only that the absolute error is small, but that there is also a large degree of cancellation of this error in evaluating the energy gap. In fact, for the energy gap the error is considerably less than the statistical uncertainty.

To obtain our best estimate for T_e , we calculated a weighted average³¹ of the energy differences for our various trial functions. The final result is $T_e = 9.4 \pm 2.2$ kcal/mole. This result is in excellent agreement with the recent experimental results of McKellar *et al.* To compare with their results we must first correct T_e for zero-point motion and relativistic effects. McKellar *et al.* assume that only the bending motion is of importance in determining the zero-point correction; however, Osamura *et al.*³² have calculated all three normal modes, and find that the stretching motion leads to a correction that is at least comparable to the bending motion. The net result is to increase the triplet state energy relative to the singlet state, and thus to reduce T_0 relative to T_e by

0.45 kcal/mole. The relativistic correction³³ amounts to a further decrease of T_0 by 0.04 kcal/mole. Thus, our best estimate for T_0 based on our QMC value for T_0 is $T_0 = 8.9 \pm 2.2$ kcal/mole. This agrees well with $T_0 = 9.05 \pm 0.06$ kcal/mole of McKellar *et al.*, and would appear to rule out the results of Refs. 6 and 7. In fact, Lineberger's new results³⁴ agree well with the present work. Furthermore, our expectation value (8.9 kcal/mole) is in closer agreement with experiment than the majority of *ab initio* calculations, though the error bars do encompass the *ab initio* values.

Note added. After this work was completed we have learned of a new review by Shavitt of the history of work on the singlet-triplet energy gap in methylene³⁵. In it is discussed a recent singles and doubles CI calculation with an exceptionally large basis set (9s6p3d2f;5s2p), using two reference configurations for the singlet, and a single reference configuration for the triplet³⁶. In this work a value of $T_0 = 9.4$ kcal/mole is obtained, in substantial agreement with the QMC result reported here. A somewhat smaller, though still large, basis set (9s7p2d1f;5s2p) gave $T_0 = 9.9$ kcal/mole^{4b}. We emphasize here the relative *insensitivity* of QMC energies to the choice of basis set, and further point out that our calculations were reliably performed with a single determinant for *both* the triplet and the singlet states.

Acknowledgments

We thank R. N. Barnett, B. Hammond, R. Grimes, and R. K. Owen for a critical reading of the manuscript.

Appendix

In Sect. III we discuss iteratively scaling the fixed-node wave function. If $\hat{\varphi}(\{r_i\})$ is a solution to the Schrödinger equation with the fixed-node boundary conditions, the question arises, is the scaled function $\hat{\varphi}(\eta\{r_i\})$ a solution to the

Schrödinger equation with scaled boundary conditions? If it is, the iterative process illustrated in Fig. 1 ends with the first line. Here we demonstrate that in general this is not the case.

Let us define the following quantities for an operator O :

$$O(\eta) \equiv \langle \hat{\varphi}(\eta\{r_i\}) | O | \hat{\varphi}(\eta\{r_i\}) \rangle / \langle \hat{\varphi}(\eta\{r_i\}) | \hat{\varphi}(\eta\{r_i\}) \rangle \quad (\text{A1})$$

and

$$\tilde{O}(\eta) \equiv \langle \Psi_T(\eta\{r_i\}) | O | \hat{\varphi}(\eta\{r_i\}) \rangle / \langle \Psi_T(\eta\{r_i\}) | \hat{\varphi}(\eta\{r_i\}) \rangle. \quad (\text{A2})$$

By the usual scaling arguments,

$$V(\eta) = \eta V(1) \quad (\text{A3})$$

$$\tilde{V}(\eta) = \eta \tilde{V}(1) \quad (\text{A4})$$

$$T(\eta) = \eta^2 T(1) \quad (\text{A5})$$

$$\tilde{T}(\eta) = \eta^2 \tilde{T}(1). \quad (\text{A6})$$

where V and T are the potential and kinetic energy operators.

Now, $E(\eta)$ and $\tilde{E}(\eta)$ are given by Eqs. (A1) and (A2) respectively, with O replaced by H . Thus,

$$E(\eta) = V(\eta) + T(\eta) = \eta V(1) + \eta^2 T(1), \quad (\text{A7})$$

and

$$\tilde{E}(\eta) = \tilde{V}(\eta) + \tilde{T}(\eta) = \eta \tilde{V}(1) + \eta^2 \tilde{T}(1). \quad (\text{A8})$$

Let us assume that $\hat{\varphi}(\eta\{r_i\})$ is indeed a solution to the Schrödinger equation with scaled boundary conditions. Then

$$H \hat{\varphi}(\eta\{r_i\}) = E_\eta \hat{\varphi}(\eta\{r_i\}). \quad (\text{A9})$$

In that case, Eqs. (A1) and (A2) both give E_η for $O=H$. That is $E(\eta) = \tilde{E}(\eta)$. By Eqs. (A7) and (A8), this can only hold for arbitrary η if $V(1) = \tilde{V}(1)$ and $T(1) = \tilde{T}(1)$. Since this is false [cf. Eqs. (A1) and (A2) for $\eta=1$], the assumption must be incorrect.

References

1. G. Herzberg and J. Shoosmith, *Nature (London)* **183**, 1801 (1959).
2. J. F. Harrison and L. C. Allen, *J. Amer. Chem. Soc.* **91**, 807 (1969).
3. M. L. Halberstadt and J. R. McNesby, *J. Amer. Chem. Soc.* **89**, 3417 (1967);
R. W. Carr, Jr., T. W. Ede, M. G. Topor, *J. Chem. Phys.* **53**, 4716 (1970).
4. (a) P. J. Hay, W. J. Hunt, and W. A. Goddard III, *Chem. Phys. Lett.* **13**, 30 (1972); (b) L. B. Harding and W. A. Goddard III, *J. Chem. Phys.* **67**, 1777 (1977); (c) S. K. Shih, S. D. Peyerimhoff, R. J. Buenker, M. Peric, *Chem. Phys. Lett.* **55**, 206 (1978); (d) C. W. Bauschlicher, Jr. and I. Shavitt, *J. Am. Chem. Soc.* **100**, 739 (1978); (e) C. W. Bauschlicher, Jr., *Chem. Phys. Lett.* **74**, 273 (1980); (f) E. R. Davidson, L. E. McMurchie, and S. Day, *J. Chem. Phys.* **74**, 5491 (1981); (g) P. Saxe, H. F. Schaefer III, and N. C. Handy, *J. Phys. Chem.* **85**, 745 (1981); (h) H.-J. Werner and E.-A. Reinsch, *J. Chem. Phys.* **76**, 3144 (1982); (i) D. Feller, L. E. McMurchie, W. T. Borden, and E. R. Davidson, *J. Chem. Phys.* **77**, 6134 (1982).
5. H. M. Frey and G. J. Kennedy, *J. Chem. Soc. Chem. Commun.* **1975**, 233 (1975); *J. Chem. Soc. Faraday Trans. I* **73**, 164 (1977).
6. P. F. Zittel, G. B. Ellison, S. V. O'Neil, E. Herbst, W. C. Lineberger, and W. P. Reinhardt, *J. Am. Chem. Soc.* **98**, 3731 (1976).
7. P. C. Engelking, R. R. Corderman, J. J. Wendoloski, G. B. Ellison, S. V. O'Neil, and W. C. Lineberger, *J. Chem. Phys.* **74**, 5460 (1981).
8. R. K. Lengel and R. N. Zare, *J. Am. Chem. Soc.* **100**, 7495 (1978).
9. C. C. Hayden, D. M. Neumark, K. Shobatake, R. K. Sparks, and Y. T. Lee, *J. Chem. Phys.* **76**, 3607 (1982).
10. A. R. W. McKellar, P. R. Bunker, T. J. Sears, K. M. Evenson, R. J. Saykally, and S. R. Langhoff, *J. Chem. Phys.* **79**, 5251 (1983).
11. L. B. Harding and W. A. Goddard III, *Chem. Phys. Lett.* **55**, 217 (1978), and

- Ref. 4d.
12. M. H. Kalos, Phys. Rev. 128, 1791 (1962); J. Comp. Phys. 1, 257 (1967).
 13. M. H. Kalos, D. Levesque, and L. Verlet, Phys. Rev. A 9, 2178 (1974).
 14. J. B. Anderson, J. Chem. Phys. 63, 1499 (1975); 65, 4121 (1976).
 15. D. M. Ceperley and M. H. Kalos, in *Monte Carlo Methods in Statistical Physics*, edited by K. Binder (Springer-Verlag, Berlin, 1979).
 16. J. B. Anderson, J. Chem. Phys. 73, 3897 (1980); F. Mentch and J. B. Anderson, J. Chem. Phys. 74, 6307 (1981).
 17. D. M. Ceperley and B. J. Alder, Phys. Rev. Lett. 45, 566 (1980).
 18. D. M. Ceperley in *Recent Progress in Many-Body Theories*, edited by J. G. Zabolitzky, M. de Llano, M. Fortes, and J. W. Clark (Springer-Verlag, Berlin, 1981).
 19. P. J. Reynolds, D. M. Ceperley, B. J. Alder, and W. A. Lester, Jr., J. Chem. Phys. 77, 5593 (1982).
 20. J. W. Moskowitz, K. E. Schmidt, M. A. Lee, and M. H. Kalos, J. Chem. Phys. 7, 349 (1982).
 21. D. M. Ceperley, J. Comp. Phys. 51, 404 (1983).
 22. P. J. Reynolds, R. N. Barnett, and W. A. Lester, Jr., Int. J. Quant. Chem. Symp. 18, xxx (1984); F. Mentch and J. Anderson, J. Chem. Phys. 80, 2675 (1984); R. N. Barnett, P. J. Reynolds, and W. A. Lester, Jr., J. Chem. Phys., *submitted*.
 23. D. M. Ceperley and B. J. Alder, J. Chem. Phys., *in press*.
 24. K. E. Schmidt and M. H. Kalos, in *Monte Carlo Methods in Statistical Physics II*, edited by K. Binder, *to be published*.
 25. N. Metropolis and S. M. Ulam, J. Am. Stat. Assoc. 44, 335 (1949).
 26. B. Holmer and D. M. Ceperley, *private communication*; B. Wells, P. J. Reynolds, and W. A. Lester, Jr., *unpublished*.
 27. R. B. Dingle, Philos. Mag. 40, 573 (1949); R. Jastrow, Phys. Rev. 98, 1479

- (1955).
28. P-O. Löwdin, in *Advances in Chemical Physics*, Vol. II, edited by I. Prigogine (Interscience, New York, 1959); E. A. Hylleraas, *Z. Physik* 54, 347 (1929).
29. In principle we would continue the iteration with $\hat{\varphi}(\eta\{r_i\})$ directly, except that we have no analytic expression for this function.
30. D. M. Ceperley, private communication.
31. The standard weighting for data with different uncertainties σ is by $1/\sigma^2$. This is what is reported. A straight average would lead to $T_e = 9.1$ kcal/mole, but is inappropriate in this context.
32. Y. Osamura, Y. Yamaguchi, and H. F. Schaefer III, *J. Chem. Phys.* 75, 2919 (1981).
33. E. R. Davidson, D. Feller, and P. Phillips, *Chem. Phys. Lett.* 76, 416 (1980).
34. D. G. Leopold, K. K. Murray, and W. C. Lineberger, *J. Chem. Phys.* 81, 1048 (1984)
35. I. Shavitt, *Tetrahedron* ("Symposium in Print") *in press*.
36. H.-J. Werner, *Habilitationsschrift*, Univ. of Frankfurt, 1982, *unpublished*, (as cited in Ref. 35.)

Table Captions

Table I. Monte Carlo energies for the 3B_1 and 1A_1 states of CH_2 , and the corresponding energy differences, obtained for three different trial wave functions Ψ_T . All three functions consist of a single determinant. The explicit forms for these functions are given in Tables IV and V. DZ denotes a double-zeta basis set; the DZ+B basis also includes an optimized $1s$ function on each C-H bond. The symbols eeJ and enJ denote electron-electron and electron-nuclear Jastrow factors respectively. The numbers in parenthesis give the statistical uncertainty in the corresponding result.

Table II. Comparison of QMC results with SCF, CI, and experimental values. The results indicated as "expt" are corrected for zero-point motion and relativistic effects to make the comparison direct. The lowest variance QMC result for T_e is not the difference of the QMC values given for the two states. Instead T_e is obtained by averaging the results of all the Ψ_T 's (cf. Table I).

Table III. Fixed-node energies obtained by iteratively scaling the 1A_1 state starting with the DZ+eeJ trial function. The eigenfunctions shown correspond to the functions in the middle column of Fig. 1. Here $\eta=1.013$ and $\eta'=1.011$.

Table IV. Trial functions Ψ_T for the 3B_1 state of CH_2 . Molecular orbitals (MO's) $\psi_1-\psi_3$ are doubly occupied. The parameters a, b , and λ, ν refer to the electron-electron and electron-nuclear Jastrow factors, which are of the form $\exp \sum_{ij} ar_{ij} / (1+br_{ij})$ and $\exp \sum_{ia} \lambda r_{ia} / (1+\nu r_{ia})$ respectively. Functions $\Psi_T^{(I)}$ and $\Psi_T^{(II)}$ use the same double-zeta basis set, but differ in that $\Psi_T^{(I)}$ lacks the electron-nuclear Jastrow factor. $\Psi_T^{(III)}$ also lacks the electron-nuclear Jastrow factor, but uses a larger basis set, which includes $1s$ functions centered along the C-H bonds. The latter were optimized for ζ as well as for the position of the

center in the plane of the molecule. The geometry of the molecule has been taken from Bauschlicher⁴⁶. Lengths are in bohr. The MO coefficients are rounded here to four places.

Table V. Trial functions Ψ_T for the 1A_1 state of CH_2 . All MO's are doubly occupied. See Table IV for a complete discussion of the symbols used.

Figure Captions

Figure 1. Schematic illustration of process for globally optimizing Ψ_T . The original trial function is $\Psi_T(\{\mathbf{r}_i\})$, while the subsequent trial functions are $\Psi_T^{(1)}$, $\Psi_T^{(2)}$, etc. The functions in the middle column are the solutions of the fixed-node Schrödinger equation, with the nodes of the Ψ_T to the left. The final functions on the right are the scaled fixed-node functions, but are no longer solutions to the Schrödinger equation. Along the path indicated by arrows, each function has a lower variational energy than that preceding it.

Table I.

Ψ_T	Energy (hartrees)		Δ_{S-T} (Kcal/mole)
	3B_1	1A_1	
DZ+eeJ	-39.1317(40)	-39.1134(35)	11.48(3.34)
DZ+eeJ+enJ	-39.1401(39)	-39.1276(28)	7.84(3.01)
DZ+B+eeJ	-39.1294(90)	-39.1167(100)	7.97(8.44)

Table II.

Method *	Energy (hartrees)		T_e (Kcal/mole)
	3B_1	1A_1	
SCF	-38.9348 ^a	-38.8944 ^b	25.4
2C-SCF	---	-38.9177 ^c	10.7 ^d
2R-CI-SD	-39.1160 ^e	-39.1003 ^e	9.9 ^e
CI-SD(Q)	-39.122 ^e	-39.105 ^e	10.7 ^e
QMC	-39.140(4)	-39.128(3)	9.4(2.2)
"expt"	-39.148 ^f	-39.133 ^g	9.55 ^h

* **Glossary of Methods**

SCF = self-consistent field

2C-SCF = two-configuration SCF

2R-CI-SD = two-reference configuration, single and double excitations CI for the singlet; one reference configuration CI-SD for the triplet.

CI-SD(Q) = singles and doubles CI, quadruples estimated.

QMC = quantum Monte Carlo (this work).

^a Ref. 4i and J. H. Meadows and H. F. Schaefer III, J. Am. Chem. Soc. 98, 4383 (1976).

^b Ref. 4g.

^c Ref. 4i.

^d using 1C-SCF for the 3B_1 state.

^e Ref. 4h.

^f Ref. 4f.

^g obtained by subtracting T_e from the "expt" energy of 3B_1 CH₂.

^h obtained from T_e of McKellar *et. al.* (Ref. 10), corrected for zero-point motion (Ref. 32) and relativistic effects (Ref. 33).

Table III.

Fixed-node eigenfunction	Energy (hartrees)
$\hat{\varphi}(\{r_i\})$	-39.113(4)
$\hat{\varphi}^{(1)}(\eta\{r_i\})$	-39.110(9)
$\hat{\varphi}^{(2)}(\eta'\eta\{r_i\})$	-39.094(9)

Table IV.

Trial Function	(a, b)	Center (x, y, z)	(λ, ν)	STO	(ζ)	MO Coefficients								
						ψ_1	ψ_2	ψ_3	ψ_4	ψ_5				
$\Psi_f^{(I)}, \Psi_f^{(II)}$	(0.5, 2.5)	C (0, 0, 0)	(0.2, 0.3)	$1s_a$	(7.52)	-0.2331	-0.0137	0	-0.0007	0				
				$1s_b$	(5.12)	-0.7767	0.2369	0	0.0999	0				
				$2s_a$	(1.83)	0.0010	-0.6341	0	-0.3472	0				
				$2s_b$	(1.15)	-0.0017	-0.0676	0	-0.2363	0				
				$2p_{x_a}$	(2.73)	0	0	-0.1985	0	0				
				$2p_{x_b}$	(1.25)	0	0	-0.4519	0	0				
				$2p_{y_a}$	(2.73)	0	0	0	0	0.2323				
				$2p_{y_b}$	(1.25)	0	0	0	0	0.8256				
				$2p_{z_a}$	(2.73)	-0.0007	-0.0646	0	0.2165	0				
				$2p_{z_b}$	(1.25)	-0.0006	-0.1377	0	0.6855	0				
						H (-1.87110, 0, 0.82525)	(0.1, 0.5)	$1s_a$	(1.64)	-0.0014	-0.1204	0.1438	-0.0211	0
								$1s_b$	(1.12)	0.0009	-0.1497	0.2217	0.2030	0
						H (1.87110, 0, 0.82525)	(0.1, 0.5)	$1s_a$	(1.64)	-0.0014	-0.1204	-0.1438	-0.0211	0
								$1s_b$	(1.12)	0.0009	-0.1497	-0.2217	0.2030	0
$\Psi_f^{(III)}$	(0.5, 2.5)	C (0, 0, 0)	---	$1s_a$	(7.52)	0.2331	-0.0119	0	-0.0005	0				
				$1s_b$	(5.12)	0.7766	0.2381	0	0.0965	0				
				$2s_a$	(1.83)	-0.0025	-0.5491	0	-0.3665	0				
				$2s_b$	(1.15)	0.0009	-0.0148	0	-0.2728	0				
				$2p_{x_a}$	(2.73)	0	0	-0.2047	0	0				
				$2p_{x_b}$	(1.25)	0	0	-0.3465	0	0				
				$2p_{y_a}$	(2.73)	0	0	0	0	0.2282				
				$2p_{y_b}$	(1.25)	0	0	0	0	0.8289				
				$2p_{z_a}$	(2.73)	0.0003	-0.0623	0	0.2157	0				
				$2p_{z_b}$	(1.25)	0.0003	-0.1011	0	0.6715	0				
						H (-1.87110, 0, 0.82525)	---	$1s_a$	(1.64)	0.0014	-0.1260	0.1343	-0.0213	0
								$1s_b$	(1.12)	-0.0018	-0.0960	0.1912	0.1946	0
						H (1.87110, 0, 0.82525)	---	$1s_a$	(1.64)	0.0014	-0.1260	-0.1343	-0.0213	0
								$1s_b$	(1.12)	-0.0018	-0.0960	-0.1912	0.1946	0
		bond (-1.13036, 0, 0.52710)	---	$1s$	(1.07)	0.0020	-0.1192	0.1447	0.0427	0				
		bond (1.13036, 0, 0.52710)	---	$1s$	(1.07)	0.0020	-0.1192	-0.1447	0.0427	0				

Table V.

Trial Function	(a, b)	Center (x, y, z)	(λ, ν)	STO	(ζ)	MO Coefficients							
						ψ ₁	ψ ₂	ψ ₃	ψ ₄				
Ψ ^(I) , Ψ ^(II)	(0.5, 2.5)	C (0, 0, 0)	(0.2, 0.3)	1s _a	(7.52)	-0.2335	0.0116	0	-0.0034				
				1s _b	(5.12)	-0.7763	-0.2335	0	-0.1020				
				2s _a	(1.83)	0.0010	0.6421	0	0.3428				
				2s _b	(1.15)	0.0002	0.1267	0	0.3255				
				2p _{x_a}	(2.73)	0	0	0.2050	0				
				2p _{x_b}	(1.25)	0	0	0.4121	0				
				2p _{z_a}	(2.73)	-0.0044	0.0693	0	-0.2018				
				2p _{z_b}	(1.25)	0.0028	0.1544	0	-0.6053				
				H (-1.64440, 0, 1.32213)	(0.1, 0.5)	1s _a	(1.64)	0.0001	0.1557	-0.0702	0.0115		
						1s _b	(1.12)	-0.0016	0.0672	-0.3639	-0.2388		
				H (1.64440, 0, 1.32213)	(0.1, 0.5)	1s _a	(1.64)	0.0001	0.1557	0.0702	0.0115		
						1s _b	(1.12)	-0.0016	0.0672	0.3639	-0.2388		
				Ψ ^(III)	(0.5, 2.5)	C (0, 0, 0)	---	1s _a	(7.52)	0.2335	-0.0113	0	0.0039
								1s _b	(5.12)	0.7762	0.2384	0	0.0968
2s _a	(1.83)	-0.0023	-0.5549					0	-0.3643				
2s _b	(1.15)	-0.0008	-0.0255					0	-0.3776				
2p _{x_a}	(2.73)	0	0					-0.2061	0				
2p _{x_b}	(1.25)	0	0					-0.3272	0				
2p _{z_a}	(2.73)	0.0037	-0.0700					0	0.2028				
2p _{z_b}	(1.25)	-0.0031	-0.0738					0	0.5754				
H (-1.64440, 0, 1.32213)	---	1s _a	(1.64)					0.0001	-0.1488	0.0826	-0.0147		
		1s _b	(1.12)					0.0009	-0.0452	0.2882	0.2351		
H (1.64440, 0, 1.32213)	---	1s _a	(1.64)					0.0001	-0.1488	-0.0826	-0.0147		
		1s _b	(1.12)					0.0009	-0.0452	-0.2882	0.2351		
bond (-0.90580, 0, 0.81559)	---	1s	(1.04)					0.0015	-0.1320	0.1768	0.0523		
		1s	(1.04)					0.0015	-0.1320	-0.1768	0.0523		

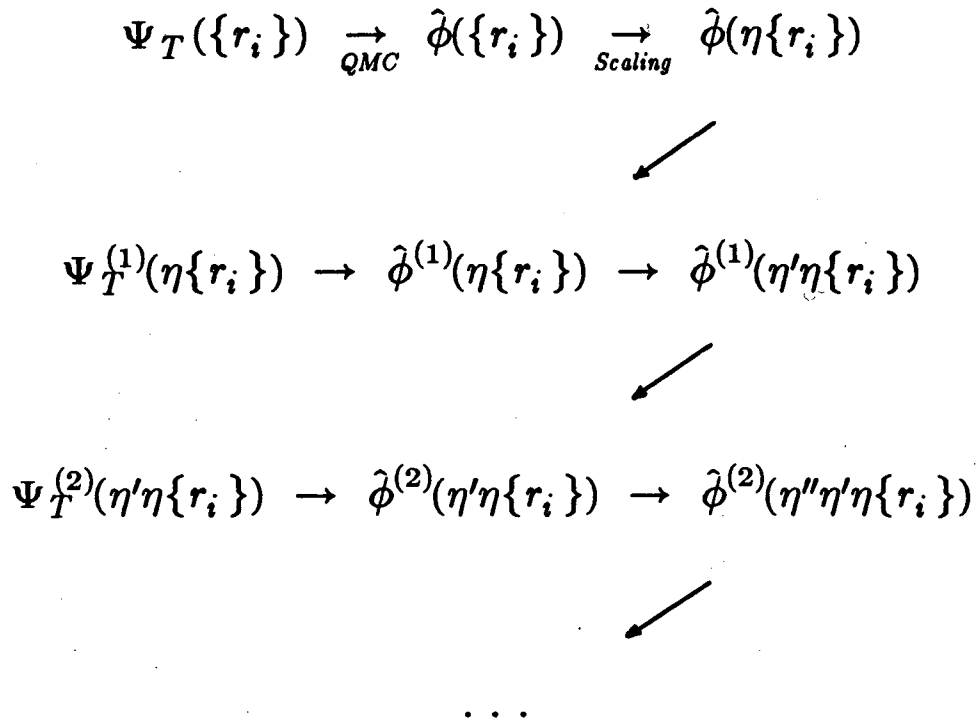


Figure 1

This report was done with support from the Department of Energy. Any conclusions or opinions expressed in this report represent solely those of the author(s) and not necessarily those of The Regents of the University of California, the Lawrence Berkeley Laboratory or the Department of Energy.

Reference to a company or product name does not imply approval or recommendation of the product by the University of California or the U.S. Department of Energy to the exclusion of others that may be suitable.

TECHNICAL INFORMATION DEPARTMENT
LAWRENCE BERKELEY LABORATORY
UNIVERSITY OF CALIFORNIA
BERKELEY, CALIFORNIA 94720